J. Fluid Mech. (1999), *vol.* 393, *pp.* 149–174. Printed in the United Kingdom

Grain sorting and bar instability

By STEFANO LANZONI[1] AND MARCO TUBINO[2]

[1]Dipartimento di Ingegneria Idraulica, Marittima e Geotecnica, Università di Padova,
Via Loredan 20, 35131 Padova, Italy
e-mail: lanzo@idra.unipd.it
[2]Dipartimento di Ingegneria Civile e Ambientale, Università di Trento,
Via Mesiano 77, 38100 Trento, Italy
e-mail: tubino@ing.unitn.it

(Received 5 January 1998 and in revised form 15 January 1999)

A two-dimensional model of flow and bed topography is proposed to investigate the effect of sediment heterogeneity on the development of alternate bars. Within the context of a linear stability theory the flow field, the bed topography and the grain size distribution function are perturbed leading to an integro-differential linear eigenvalue problem. It is shown that the selective transport of different grain size fractions and the resulting spatial pattern of sorting may appreciably affect the balance between stabilizing and destabilizing actions which govern bar instability. Theoretical results suggest that sediment heterogeneity leads to a damping of both growth rate and migration speed of bars, while bar wavelength is shortened with respect to the case of uniform sediment. The above findings conform, at least qualitatively, to the experimentally detected reduction of bar height, length and celerity. The observed tendency of coarser particles to pile up towards bar crests is also reproduced by theoretical results.

1. Introduction

Alternate bars are the most common type of large-scale bedforms which are observed both in sandy streams and in gravel bed rivers. They essentially consist of migrating alternating regions of scour and deposit with horizontal scale of the order of several channel widths and vertical scale of the order of the flow depth. Their vertical spatial scale being so large, the problem of predicting their occurrence and their equilibrium characteristics has a profound impact on several aspects of river engineering.

A fairly consistent picture of the process underlying bar development in cohesionless channels has been built up through a large number of theoretical and experimental works, which have been mainly developed in the last two decades. In particular, it has been progressively established that the occurrence of bars and their response to the planimetric evolution of channels are crucial ingredients required to characterize the overall morphology of alluvial channels at the river reach scale (see the state of the art reviews of Seminara & Tubino 1989, and Seminara 1995).

The formation of river bars has been conclusively explained in terms of an inherent instability of an erodible bed subject to a turbulent flow in straight channel, which enables the growth of infinitesimal flow and bottom perturbations migrating downstream. Several increasingly refined two-dimensional linear stability theories are available in the literature for the case when the dominant form of sediment transport

is bedload (see e.g. Callander 1969; Parker 1976; Fredsöe 1978; Colombini, Seminara & Tubino 1987; Garcia & Niño 1993). These theories allow one to predict the growth rate of perturbations within the linear regime, the marginal stability conditions in the space of flow and sediment parameters and the wavelength and wave speed selected by the instability mechanism, i.e. those corresponding to the maximum growth rate. In particular, it appears that in bedload dominated channels the width to depth ratio β is the control parameter of bar instability such that a threshold value β_c can be determined, for given Shields parameter Θ and relative grain roughness d_s, above which bars are expected to grow. The balance between stabilizing and destabilizing actions yielded by linear theory also suggests that the alternate bar mode is the most unstable, the higher modes (leading for example to central or multiple bar configurations) prevailing only for values of β which are much larger than the threshold value.

Furthermore, Colombini *et al.* (1987) and Colombini & Tubino (1991) have investigated nonlinear interactions of various modes arising when β exceeds the threshold value, showing that nonlinear effects cause bed perturbations to reach an equilibrium finite amplitude characterized by periodic diagonal fronts. Under suitable conditions, which are rarely encountered in nature, the above equilibrium solution may in turn become unstable and bifurcate into a more complex quasi-periodic pattern (Schielen, Doelman & De Swart 1993).

Whether the width-to-depth ratio keeps the role of control parameter of bar instability when suspended load prevails, i.e. in sandy streams, is still an open question. Suspended load has been found to be invariably destabilizing, i.e. enhancing bar development, by Fredsöe (1978) and Kuroki (1988); on the other hand, Watanabe & Tubino's (1992) results suggest that for given grain size a threshold value of Shields stress (i.e. of suspended load intensity) exists above which bar perturbations are suppressed, the critical value β_c becoming infinite. Furthermore, the three-dimensional analysis of Repetto, Tubino & Zolezzi (1996) introduces a more subtle mechanism of suppression of alternate bars in that it is found that suspension enhances the occurrence of higher transverse modes which may then take over even for relatively low values of β.

The analyses on river bars mentioned above have concentrated on the case of uniform sediment. This is partly motivated by the complexity and cost of laboratory work on sediment mixtures, especially when dealing with large-scale features which involve a considerable amount of sediments. Furthermore, significant progress in obtaining knowledge of the physical mechanisms underlying bedload transport of sediment mixtures has been achieved only quite recently (see the extensive review of Parker 1992).

Nevertheless, the mixed character of the sediment is a significant characteristic of river beds, particularly of gravel bed rivers. A wide range of features of gravel rivers cannot be adequately explained without reference to the entire particle size distribution as well as to the related morphological characteristics of gravel beds (armouring, vertical sorting). The selective transport of individual size fractions of a mixture, which is induced by bed deformation and spatial non-uniformity of bed shear stress distribution, results in a consistent pattern of longitudinal and transverse sorting which in turn affects the balance between stabilizing and destabilizing effects controlling bedform development. This is suggested by several field and flume data (Lisle, Ikeda & Iseya 1991; Diplas & Parker 1992; Lisle & Madej 1992; Ashworth, Ferguson & Powell 1992*b*; Lanzoni 1996). Furthermore, field observations of Whiting *et al.* (1985) and theoretical results of Seminara, Colombini & Parker (1996) suggest

that there exists a class of morphological patterns (called bedload sheets) which are inherently associated with the heterogeneous character of the sediment and may be the cause of temporal and spatial variations of bedload transport typical of gravel rivers.

The above considerations strongly motivate the need to investigate the role of sediment heterogeneity on bar instability. The basic questions to be answered are: How does the heterogeneous character of sediment affect the mechanism which gives rise to bars in the uniform case? What is the spatial distribution of different grain sizes induced by bar development? Does sediment non-uniformity introduce in the stability analysis further ingredients which are inherently associated with particle size distribution? Indeed, the spatial variations of both bottom roughness, which are induced by sorting, and of bedload transport, which are triggered by the deviation from equal mobility of different sizes, constitute additional mechanisms able to modify the instability process with respect to the case of uniform sediment.

From the technical point of view the fundamental question posed by the mixed character of sediments is that of ascertaining whether the region of bar occurrence and the depth of scour and depositional regions change when sediment heterogeneity is taken into account. Experimental findings seem to suggest that the topography of bars is significantly modified. In particular, sediment non-uniformity has been found to induce a somewhat episodic bar growth, even under steady hydraulic conditions, and to prevent downstream migration of bars by inhibiting sediment transport over them (Lisle *et al.* 1991). Moreover, depending on the average Shields stress and relative bed roughness, a significant reduction of bar amplitude and change of bar wavelength have been detected compared to the case of uniform sediment (Lanzoni, Tubino & Bruno 1994; Lanzoni 1996).

In the present investigation a suitable treatment of sediment mixtures, whereby the model of Parker (1990) is adopted along with Hirano's (1971) concept of active layer, is incorporated within the framework of a linear stability analysis of flow and bottom topography. Since sediment heterogeneity mainly characterizes gravel bed rivers, we neglect suspended load. Therefore a simple two-dimensional description of flow and sediment transport is adopted.

A similar stability analysis for the grain size distribution has been recently proposed by Seminara *et al.* (1996) to explain the formation of bedload sheets. The most noticeable difference introduced by the present work is that the full coupling between perturbations of bottom topography and grain size distribution is retained.

The main output of the theory is a significant damping of bar instability, which is implied by the decrease of the growth rate of bar perturbations for increasing values of the standard deviation of sediment mixture. On the other hand, the critical value of width ratio for the occurrence of bars does not seem to be significantly affected by the heterogeneous character of the sediment, the values of β_c falling slightly above or below those obtained in the uniform case depending on the dimensionless grain roughness.

Furthermore, theoretical results suggest that the pattern of sorting which is induced by the development of bottom topography crucially depends on the relative importance of the mechanisms which are responsible for the spatial displacement of particles. In particular, while gravitational effects tend to pull selectively coarser particles downward, the unequal response of grain sizes to spatial variations of bottom stress seems to promote the piling up of coarser particles towards bar crests. When the spatial variations of bottom topography are relatively slow, as in the case of river bars, the latter mechanism seems to prevail leading to the progressive coarsening which is often observed along the upstream face of bars.

Further related questions regarding the effect of grain sorting on the equilibrium amplitude of bars will require additional investigation where nonlinear effects are accounted for.

The rest of the paper is organized as follows. In § 2 we formulate the problem. The linear stability analysis is reported in § 3, while in § 4 we derive an analytical solution of the dispersion relationship arising from linear theory for the case when the average grain size distribution function is represented in terms of Dirac distributions. Finally, § 5 contains a discussion of the results along with some concluding remarks.

2. Formulation of the problem

Let us consider the flow in a straight alluvial channel with non-erodible banks and constant width $2B^*$ large enough for the flow to be modelled as two-dimensional. The channel bottom is assumed to be made up of a mixture of cohesionless sediments of density ρ_s. The probability density function describing the distribution of grain sizes available for bedload transport which are contained within the surface layer is denoted by $f(\phi, s^*, n^*, t^*)$. Here ϕ is the sedimentological scale for particle size defined such that the grain diameter (in mm) is $d^* = 2^{-\phi}$, s^* and n^* are the longitudinal and transverse Cartesian coordinates and t^* is time (here and in the following a star superscript denotes dimensional quantities).

The first preliminary question which needs to be addressed is that of selecting a suitable model for the probability density function f. Plots of cumulative frequencies of grain size distributions of sediments transported in nature versus the logarithms of grain sizes are generally line segments. A common explanation of this behaviour is that these segments result from log-normal subpopulations that are either truncated or overlapped (Visher 1969; Tanner 1983), each transported by a particular mechanism (bedload, saltation, suspended load). Nevertheless, sediments transported by a single mechanism may also display segmented patterns since a prolonged transportation as bedload or suspended load is required to let the grain size distribution become nearly perfectly log-normal (Sengupta, Ghosh & Mazumder 1991). Quite often grain size distributions of natural sediments are found to fit a log-hyperbolic distribution (Bagnold & Barndorff-Nielsen 1980) or a bimodal distribution (Shaw & Kellerhals 1982). Estimation of the four parameters needed for the specification of a hyperbolic distribution, however, is rather complicated as discussed in Christiansen & Hartman (1991). Therefore, in the following we will assume that the gross features of the grain size distribution can be adequately described by the first and second moments of the distribution. Hence we can write

$$\phi_g = \int_{-\infty}^{\infty} f\phi \, \mathrm{d}\phi, \qquad \sigma^2 = \int_{-\infty}^{\infty} (\phi - \phi_g)^2 f \, \mathrm{d}\phi, \tag{2.1a,b}$$

which allow us to define the geometric mean grain diameter $d_g^* = 2^{-\phi_g}$ and its standard deviation $\sigma_g = 2^{\sigma}$, respectively. By definition the probability density function is subject to the following integral condition:

$$\int_{-\infty}^{\infty} f(\phi, s^*, n^*, t^*) \, \mathrm{d}\phi = 1. \tag{2.2}$$

It is worth pointing out that the use of a probability density function f which is independent of the vertical coordinate rules out the possibility of taking into account the effect of vertical sorting on bar development. The above assumption, which goes back to the original formulation of the Exner equation for size fractions introduced

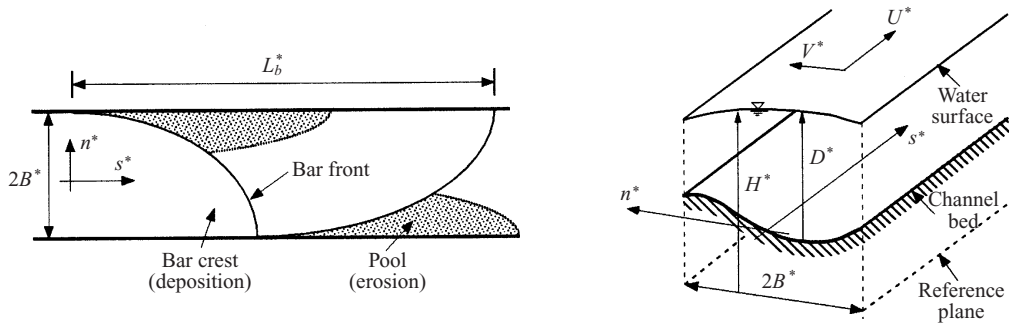

FIGURE 1. Sketch of the channel and notation.

by Hirano (1971) and has been successfully employed by Seminara *et al.* (1996) to explain the formation of gravel sheets, may only be justified in the case of bedforms with negligible vertical scale, while it may result into a too crude approximation when applied in a context in which bedform development and migration act significantly to mix the sediment within the bed layer. The case of dunes in heterogeneous sediments is a notable example where vertical sorting may play a significant role (see Ribberink 1987). Some recent attempts to characterize vertical sorting through a continuous vertical size distribution are documented in the literature (see e.g. Armanini 1995). However, since we are concerned with the process of incipient formation of bars we may discard this effect, which greatly simplifies the theoretical treatment. Moreover, unlike in the dune case, here the relevant spatial scale of flow and bottom non-uniformity is channel width which is typically much larger than flow depth.

We wish to analyse how the flow field responds to simultaneous two-dimensional infinitesimal perturbations both of the grain size distribution and of the bottom configuration, assuming that the fluid can adapt instantaneously to such perturbations. Our basic state is a uniform flow over a flat cohesionless bed, with flow depth D_0^* and average speed U_0^*, characterized by a grain size probability density function $f_0(\phi)$. Let d_{g0}^* denote the geometric mean grain size of such a distribution, which is uniformly distributed in space. The effect of lateral distribution of grain size, such as that associated with the presence of discrete patches (Paola & Seal 1995), can be accounted for by setting a suitable initial distribution. Also, note that the influence of local composition on grain mobility is felt through the dependence of the hiding function on local mean grain diameter (see equation (2.15) below).

The formulation of the problem for the flow follows closely the work of Colombini *et al.* (1987) and will only briefly be recalled here. A steady two-dimensional formulation is adopted in as much as spatial variations occur on planimetric scales much larger than the flow depth and bedforms develop quite slowly. Sidewall layers are ignored and replaced by the condition of vanishing transverse component of the depth-averaged velocity.

The governing equations for the flow then read

$$UU_{,s} + VU_{,n} = -H_{,s} - \beta\,\tau_s/D, \tag{2.3a}$$

$$UV_{,s} + VV_{,n} = -H_{,n} - \beta\,\tau_n/D, \tag{2.3b}$$

$$(UD)_{,s} + (VD)_{,n} = 0, \tag{2.3c}$$

where (U, V) is the depth-averaged velocity vector, H is the free-surface elevation,

(τ_s, τ_n) are longitudinal and transverse components of bottom shear stress and D is the local flow depth (see figure 1). The variables have been made dimensionless in the form

$$(U^*, V^*) = U_0^*(U, V), \quad (D^*, H^*) = D_0^*(D, F_r^2 H), \tag{2.4a,b}$$

$$(s^*, n^*) = B^*(s, n), \quad (\tau_s^*, \tau_n^*) = \rho U_0^{*2}(\tau_s, \tau_n), \tag{2.4c,d}$$

where ρ is fluid density, F_r is the Froude number of uniform basic flow, and the width ratio β is:

$$\beta = B^*/D_0^*. \tag{2.5}$$

Closure of (2.3a, c) requires a suitable constitutive relationship for bottom stress. We thus express the shear stress in terms of a friction coefficient C defined by the relationship

$$(\tau_s, \tau_n) = C(U, V)(U^2 + V^2)^{1/2}. \tag{2.6}$$

The structure of C strongly depends on the presence of small-scale (ripples) and/or mesoscale (dunes) bedforms which are often found to coexist with alternate bars, particularly in sandy rivers. Here we restrict attention to gravel bed rivers in which, although the bottom may contain a certain amount of sand, bedload is dominant and dunes are less important. Incidentally, note that some experimental evidence exists which suggests that dune height tends to be damped due to sorting effects (Klaassen 1990; Lanzoni 1996).

Assuming local equilibrium we can express C in terms of the local roughness using the following relationship:

$$C^{-1/2} = 6 + 2.5 \ln (D/k_s), \tag{2.7}$$

which strictly applies to uniform conditions and a plane bed, where the dimensionless grain roughness height (scaled by D_0^*)

$$k_s = n_\sigma d_\sigma \tag{2.8}$$

is taken to be proportional to a coarse grain size defined as $d_\sigma^* = d_g^* 2^\sigma$, the constant of proportionality n_σ being roughly equal to 2 (Parker 1992).

It is worth pointing out that through the above definition of local roughness the heterogeneous character of the sediment introduces a first novel feature in the stability problem in that perturbations of the (local) average grain size, which are induced by sorting effects associated with bar development, produce through equation (2.6) perturbations of bottom stress. Whether the above effect is able to enhance or damp bar instability can only be ascertained through the determination of the sorting pattern associated with bar topography. We will see that in the case of bars the progressive coarsening observed along the upstream face of bedforms produces a local increase of roughness there, i.e. of shear stress, whose effect cumulates with the perturbed distribution of longitudinal stress typical of bars with uniform sediment.

Finally, we require that the sidewalls must be impermeable to the fluid; hence we write

$$V = 0 \quad (n = \pm 1). \tag{2.9}$$

The mathematical problem governing the motion of the fluid is then coupled to the conservation equations for the sediment. The formulation of the problem of transport and mass balance of each size fraction within the mixture follows closely that of Seminara *et al.* (1996). Therefore we will simply summarize it (see also Parker 1992).

We assume that sediments available for transport are contained in a surface-active layer (Hirano 1971) which is taken to be initially well mixed so that the probability density function f of the material within it has neither a vertical structure nor a longitudinal or a transverse structure.

The governing equations for the motion of the sediment mixture are: a statement of mass balance for each size fraction, which allows for variation of bottom elevation in time and transverse variations of bedload transport; a dynamic equation to specify the bedload transport rate of each fraction. The former reads

$$f\eta_{,t} + L_a f_{,t} + [(fQ_s)_{,s} + (fQ_n)_{,n}] = 0, \tag{2.10}$$

where $\eta = (F_r^2 H - D)$ is the dimensionless bottom elevation and (Q_s, Q_n) is a bedload vector of modulus Φ such that $f\Phi$ is the dimensionless volumetric discharge per unit width of grains in the size range $\phi, \phi + \mathrm{d}\phi$. Quantities in (2.10) are made dimensionless in the form

$$(\eta^*, L_a^*) = D_0^*(\eta, L_a), \quad t^* = t(1-p)D_0^* B^*/Q_0, \tag{2.11a,b}$$

$$(Q_s^*, Q_n^*) = Q_0(Q_s, Q_n), \quad \Delta = \frac{\rho_s}{\rho} - 1, \quad Q_0 = (\Delta g)^{1/2} d_{g0}^{*3/2}, \tag{2.11c–e}$$

where p is the porosity of the mixture and g is gravity. The thickness L_a^* of the active layer is taken to be proportional to a typical coarse grain size, namely d_σ^*. Recalling equation (2.8) we will assume in the following $L_a = k_s$, pointing out, however, that this assumption is only justified in the initial phase of bar growth since it neglects the effect of bar migration on the sediment exchange with the bed layer.

To complete the formulation we need dynamic relationships to specify bedload intensity and the direction of trajectories that particles follow due to the combined effect of bottom shear stress and gravity. Following Parker (1990) we express the sediment load function Φ as

$$\Phi = \Theta_g^{3/2} G(\zeta) \tag{2.12}$$

where ζ is a dummy variable and

$$\Theta_g = \frac{\tau^*}{\rho \Delta g d_{g0}^*} \tag{2.13}$$

denotes the dimensionless bed shear stress (Shields parameter) based on the geometric mean diameter d_{g0}^*. Several empirical predictors of the transport capacity function $G(\zeta)$ are available in the literature. In the following we will adopt the function proposed by Parker (1990), which is based on field data from Oak Creek River, where the dummy variable ζ is given the form

$$\zeta = \omega \frac{\Theta_g}{\Theta_r} \frac{d_{g0}^*}{d_g^*} g_{hr}\left(\frac{d^*}{d_g^*}\right), \tag{2.14}$$

and $\Theta_r = 0.0386$ is a reference Shields stress, g_{hr} is a reduced hiding function (Diplas 1987; Andrews & Parker 1987; Parker 1990) which adjusts the mobility of size d^* relative to d_g^*, and ω is a straining function introduced to account for the effect of the standard deviation of the grain size distribution on the transport rate of each size fraction (Parker 1990).

Field data and laboratory investigations suggests the following form of g_{hr}:

$$g_{hr} = (d_i^*/d_g^*)^{-b}, \tag{2.15}$$

Author	source of data	b
Parker & Klingeman (1982)	Oak Creek river	0.06
Parker & Klingeman (1982)	Oak Creek river	0.02[a]
White and Day (1982)	Recirculating flume	0.19
Misri, Garde & Ranga Raju (1984)	Recirculating flume	0—0.08
Andrews & Erman (1986)	Sagehen Creek	0.13[b]
Wilcock (1987)	Recirculating flume	0—0.03
Ashworth & Ferguson (1989)	Feshie and Dubhaig rivers	0.33–0.35
Ashworth & Ferguson (1989)	Lyngdalselva river	0.08
Ferguson, Prestegaard & Ashworth (1989)	White river	0.12[b]
Parker (1990)	Oak Creek river	0.10
Ashworth *et al.* (1992*a*)	Sunwapta river	0.21
Kuhnle (1992)	Goodwin Creek river	0.19[a,c]
Wilcock (1992)	Recirculating flume	0.27[d]
Wilcock & McArdell (1993)	Recirculating flume	0.55[e]
Ferguson (1994)	Roaring river	0.13[b]
Wathen *et al.* (1995)	Allt Dubhaig river	0.30[b]
Wathen *et al.* (1995)	Allt Dubhaig river	0.10

[a] Critical stress based on subsurface grain size distribution.
[b] Critical stress inferred from maximum clast size.
[c] Mixed gravel and sand bed.
[d] Strongly bimodal mixture.
[e] Very poorly sorted, bimodal mixture.

Unless otherwise specified with a superscript the critical stress and, hence, the hiding factor b, are inferred from fractional transport rates and are based on surface grain size distribution.

TABLE 1. Hiding exponent obtained from laboratory and field data.

with the exponent b ranging between 0 and 0.55 (see table 1). As pointed out by Buffington & Montgomery (1997) the variability of the exponent b, which is basically a consequence of different methods adopted to estimate the critical stress, also reflects the role of various factors related both to sediment characteristics, and to experimental procedure and data analysis. In particular, significant departures from equal mobility (i.e. $b = 0$) are documented in the case of strongly bimodal mixtures (Kuhnle 1992; Wilcock 1992; Wilcock & McArdell 1993).

We set

$$(Q_s, Q_n) = (\cos\delta, \sin\delta)\Phi \tag{2.16}$$

with δ denoting the angle which the direction of bedload transport makes with the s-direction. Investigations on the direction of bedload transport of uniform sediments in the presence of weak spatial variations of the direction of bottom shear stress and slow spatial variations of bottom elevation (Kikkawa, Ikeda & Kitagawa 1976; Ikeda 1982; Parker 1984; Olesen 1987; Sekine & Parker 1992; Talmon, Struiksma & van Mierlo 1995) suggest a prediction for δ of the form

$$\sin\delta = \sin\chi - \frac{r}{\beta\Theta^{1/2}}\eta_{,n} \tag{2.17}$$

where χ is the angle that the bottom stress vector makes with the s-axis and the parameter r ranges between 0.5 and 1.5.

Formula (2.17) can be generalized to mixtures, following the lead of Parker & Andrews (1985). Since coarser grains feel a larger ratio of transverse component

of gravitational force to downstream drag force than finer grains, it follows that coarser grains move preferentially downslope. The above effect can be accounted for by introducing a suitable weighting function f_{hr} in equation (2.17) such that the trajectory of particles of size d^* is defined in terms of the expression

$$\sin\delta = \sin\chi - \frac{r}{\beta}\left[\frac{1}{\Theta_g} f_{hr}^{-1}\left(\frac{d^*}{d_g^*}\right)\right]^{1/2}\eta_{,n}, \tag{2.18}$$

where we use the reduced hiding function f_{hr} proposed by Egiazaroff (1965), as modified by Ashida & Michiue (1972), namely

$$f_{hr}^{-1}(d^*/d_g^*) = \begin{cases} (d^*/d_g^*)(1 + 0.782\log d^*/d_g^*)^{-2}, & d^*/d_g^* \geqslant 0.4 \\ 0.843, & d^*/d_g^* < 0.4. \end{cases} \tag{2.19}$$

Finally, in order to complete the formulation for the sediment transport we must require the sidewalls to be impermeable to the sediment; hence we write

$$Q_n = 0 \quad (n = \pm 1). \tag{2.20}$$

In the next section the above formulation will be the basis for a linear stability analysis of uniform configuration.

3. Linear theory

We want to investigate the linear response of the flow field to infinitesimal perturbations of bottom configuration and grain size distribution. Therefore we perturb our basic state (the uniform flow and the uniformly distributed probability density function of grain size) and introduce the following representation of the flow field and grain size distribution:

$$(U, V, D, H) = (1, 0, 1, H_0) + \varepsilon\,(U_1(s,n,t), V_1(s,n,t), D_1(s,n,t), H_1(s,n,t)) + O(\varepsilon^2), \tag{3.1a}$$

$$f = f_0(\phi) + \varepsilon f_1(\phi, s, n, t) + O(\varepsilon^2), \tag{3.1b}$$

with ε small parameter (strictly infinitesimal). The above expansion implies that a similar representation can be used to express the longitudinal and transverse components of bedload and bottom stress, namely

$$(Q_s, Q_n, \tau_s, \tau_n) = (\Phi_0, 0, C_0, 0) + \varepsilon(Q_{s1}(\phi,s,n,t), Q_{n1}(\phi,s,n,t), \tau_{s1}(\phi,s,n,t), \tau_{n1}(\phi,s,n,t)) + O(\varepsilon^2), \tag{3.2}$$

where Φ_0 and C_0 denote the bedload function and the friction coefficient of the undisturbed uniform configuration.

Furthermore we write

$$(\phi_g, \sigma) = (\phi_{g0}, \sigma_0) + \varepsilon\,(\phi_{g1}(s,n,t), \sigma_1(s,n,t)) + O(\varepsilon^2), \tag{3.3a}$$

$$(\eta, L_a) = (0, L_{a0}) + \varepsilon\,(\eta_1(s,n,t), L_{a1}(s,n,t)) + O(\varepsilon^2) \tag{3.3b}$$

where

$$\phi_{g0} = \int_{-\infty}^{\infty} f_0 \phi\,\mathrm{d}\phi, \quad \sigma_0^2 = \int_{-\infty}^{\infty} (\phi - \phi_{g0})^2 f_0\,\mathrm{d}\phi, \tag{3.4a,b}$$

$$\phi_{g1} = \int_{-\infty}^{\infty} f_1 \phi \, \mathrm{d}\phi, \quad \sigma_1 = \frac{1}{2\sigma_0} \int_{-\infty}^{\infty} (\phi - \phi_{g0})^2 f_1 \, \mathrm{d}\phi. \tag{3.4c,d}$$

On substituting from (3.1*a*), (3.3) into the flow equations (2.3*a–c*) and performing linearization at $O(\varepsilon)$ we obtain the following differential system:

$$U_{1,s} + H_{1,s} + \beta(\tau_{s1} - C_0 D_1) = 0, \quad V_{1,s} + H_{1,n} + \beta\tau_{n1} = 0, \quad U_{1,s} + V_{1,n} + D_{1,s} = 0, \tag{3.5a–c}$$

where, using the relationships (2.6), (2.7) and (2.8), the longitudinal and transverse components of bottom shear stress can be expressed in the form

$$\tau_{s1} = C_0\{(2U_1 + D_1 C_D) + t_\phi \phi_{g1} + t_\sigma \sigma_1\}, \quad \tau_{n1} = C_0 V_1, \tag{3.6a,b}$$

with

$$t_\phi = -t_\sigma = -d_{\sigma 0} C_d \ln 2, \quad d_{\sigma 0} = d_{g0} 2^{\sigma_0}, \quad d_{g0} = 2^{-\phi_{g0}}, \tag{3.7a–c}$$

$$C_0 = C(1, d_{\sigma 0}), \quad C_D = \frac{1}{C_0} C_{,D}|_{1,d_{\sigma 0}}, \quad C_d = \frac{1}{C_0} C_{,d_g}|_{1,d_{\sigma 0}}, \tag{3.7d–f}$$

where d_{g0} denotes the undisturbed value of dimensionless geometric mean size while the subscript $(1,\ d_{\sigma 0})$ implies that functions are evaluated with reference to the unperturbed uniform state, namely with $D = 1$ and $d_\sigma = d_{\sigma 0}$.

It is worth noting that in equation (3.6*a*) the effect of sorting on bed shear stress is explicitly accounted for through the dependence of τ_{s1} on the perturbed values (ϕ_{g1}, σ_1) of the first and the second moments of grain size distribution, whence local variations of grain size distribution induce variations of local roughness which are felt by the fluid at a linear level as variations of longitudinal stress. The above effect has been found to play a crucial role in determining bedload sheet instability (Seminara *et al.* 1996), while here it plays only a complementary role since the full coupling between perturbations of bottom topography and grain size distribution has been retained; furthermore, while in the case of bedload sheets the role of free instabilities related to sediment heterogeneity is dominant, in our case perturbations of grain size distribution are mainly driven by perturbations of bottom topography. We will see that the balance between the effect of bottom perturbation and that of grain size perturbation on the longitudinal stress crucially depends on the phase lag of d_g relative to bottom elevation.

The stability analysis then proceeds with the sediment balance equation at $O(\varepsilon)$, which reads

$$f_0(F_r^2 H_{1,t} - D_{1,t}) + L_{a0} f_{1,t} + \{(\Phi_0 f_1 + Q_{s1} f_0)_{,s} + (Q_{n1} f_0)_{,n}\} = 0. \tag{3.8}$$

Linearity implies that only the unperturbed value of the thickness of the active layer $L_{a0} = n_\sigma d_{\sigma 0}$ appears in equation (3.8). The argument ζ of the function G (see (2.12), (2.14)) can be expanded in the form

$$\zeta = \zeta_0\{1 + \varepsilon[(2U_1 + D_1 C_D)(1 + \omega_T) + \zeta_\phi \phi_{g1} + \zeta_\sigma \sigma_1] + O(\varepsilon^2)\}, \tag{3.9}$$

with

$$\zeta_0 = \omega_0 \frac{\Theta_{g0}}{\Theta_r} 2^{b(\phi - \phi_{g0})}, \quad \zeta_\phi = (1 - b)\ln 2 + t_\phi(1 + \omega_T), \quad \zeta_\sigma = t_\sigma(1 + \omega_T) + \omega_\sigma \tag{3.10a–c}$$

and

$$\omega_0 = \omega(\sigma_0, \Theta_{g0}), \quad \omega_\sigma = \left[\frac{1}{\omega}\frac{\partial\omega}{\partial\sigma}\right]_{\sigma_0,\Theta_{g0}}, \quad \omega_T = \frac{\Theta_{g0}}{\Theta_r}\left[\frac{1}{\omega}\frac{\partial\omega}{\partial T}\right]_{\sigma_0,\Theta_{g0}}, \tag{3.11a–c}$$

where b is the exponent of the reduced hiding function (2.15), Θ_{g0} is Shields parameter of the basic unperturbed flow and the subscript (σ_0, Θ_{g0}) indicates that quantities are evaluated with the unperturbed values of standard deviation and Shields stress.

Combining (2.16) and (2.18), and recalling the relationships (3.6) and (3.9), the $O(\varepsilon)$ longitudinal and transverse components of bedload discharge are expressed in the form

$$Q_{s1} = \Phi_0\{(2U_1 + D_1 C_D)q_\eta + q_\phi \phi_{g1} + q_\sigma \sigma_1\}, \quad Q_{n1} = \Phi_0\{V_1 - R(F_r^2 H_{1,n} - D_{1,n})\} \tag{3.12a,b}$$

where

$$q_\eta = \tfrac{3}{2} + (1 + \omega_T)\Gamma, \quad q_\phi = \tfrac{3}{2}t_\phi + \zeta_\phi\,\Gamma, \quad q_\sigma = \tfrac{3}{2}t_\sigma + \zeta_\sigma\,\Gamma \tag{3.13a–c}$$

$$\Phi_0 = \Theta_{g0}^{3/2} G(\zeta_0), \quad \Gamma = \left[\frac{\zeta}{G}\frac{\mathrm{d}G}{\mathrm{d}\zeta}\right]_{\zeta=\zeta_0}, \quad R = \frac{r}{\beta(\Theta_{g0} f_{hr})^{1/2}}. \tag{3.13d–f}$$

The complex coefficients q_η, q_ϕ, q_σ represent the perturbations of longitudinal bedload associated with variations of the flow field induced by bottom perturbations and by the variations of the mean and the variance of grain size distribution.

Linearity of the problem allows us to perform a normal mode analysis of the perturbations by assuming

$$(U_1, D_1, H_1) = (\hat{U}_1(t), \hat{D}_1(t), \hat{H}_1(t)) \sin(\tfrac{1}{2}\pi n) \exp(\mathrm{i}\alpha s) + \text{c.c.}, \tag{3.14a}$$

$$V_1 = \hat{V}_1(t) \cos(\tfrac{1}{2}\pi n) \exp(\mathrm{i}\alpha s) + \text{c.c.}, \tag{3.14b}$$

$$(f_1, \phi_{g1}, \sigma_1) = (\hat{f}_1(\phi, t), \hat{\phi}_{g1}(t), \hat{\sigma}_1(t)) \sin(\tfrac{1}{2}\pi n) \exp(\mathrm{i}\alpha s) + \text{c.c.}, \tag{3.14c}$$

with α dimensionless wavenumber (scaled with $1/B^*$) and c.c. denoting the complex conjugate of a complex number. For clarity only the first mode in the transverse direction is considered in (3.14*a–c*) and in the following. The general form of the solution which accounts for any other transverse modes can be readily obtained.

On substituting from (3.14*a,b*) into (3.5) the differential system governing the flow field is transformed into the following linear homogeneous algebraic system:

$$\sum_{j=1}^{3} [a_{j1}\hat{U}_1 + a_{j2}\hat{V}_1 + a_{j3}\hat{H}_1 + a_{j4}\hat{D}_1 + a_{j5}(\hat{\phi}_{g1} - \hat{\sigma}_1)] = 0, \tag{3.15}$$

where

$$a_{11} = \mathrm{i}\alpha + 2\beta C_0, \qquad a_{12} = a_{21} = a_{24} = a_{25} = a_{33} = a_{35} = 0, \tag{3.16a,b}$$

$$a_{13} = a_{31} = a_{34} = \mathrm{i}\alpha, \quad a_{23} = -a_{32} = \tfrac{1}{2}\pi, \tag{3.16c,d}$$

$$a_{14} = \beta C_0(C_D - 1), \qquad a_{15} = -\beta C_0 d_\sigma C_d \ln 2, \tag{3.16e,f}$$

$$a_{22} = \mathrm{i}\alpha + \beta C_0. \tag{3.16g}$$

Using (3.15) and recalling that (3.14*a*) implies that the bottom perturbation has a

similar structure, with $\hat{\eta}_1 = F_r^2\hat{H}_1 - \hat{D}_1$, we can readily express $\hat{U}_1, \hat{V}_1, \hat{D}_1, \hat{H}_1$ in the form

$$[\hat{U}_1, \hat{V}_1, \hat{H}_1, \hat{D}_1] = (b_{10}, b_{20}, b_{30}, b_{40})\hat{\eta}_1 + (b_{11}, b_{21}, b_{31}, b_{41})(\hat{\phi}_{g1} - \hat{\sigma}_1), \tag{3.17}$$

with

$$b_{10} = -\frac{1}{\mathrm{i}\alpha F_r^2 - P_0}\left(P_0 + \frac{\pi^2}{4}\frac{1}{a_{22}}\right), \quad b_{11} = -\frac{P_1}{\mathrm{i}\alpha F_r^2 - P_0}\left(\mathrm{i}\alpha F_r^2 + \frac{\pi^2}{4}\frac{1}{a_{22}}\right), \tag{3.18a,b}$$

$$b_{20} = -\frac{\pi}{2}\frac{\mathrm{i}\alpha}{a_{22}}\frac{1}{\mathrm{i}\alpha F_r^2 - P_0}, \qquad b_{21} = -\frac{\pi}{2}\frac{\mathrm{i}\alpha}{a_{22}}\frac{P_1}{\mathrm{i}\alpha F_r^2 - P_0}, \tag{3.18c,d}$$

$$b_{30} = \frac{\mathrm{i}\alpha}{\mathrm{i}\alpha F_r^2 - P_0}, \qquad b_{31} = \frac{\mathrm{i}\alpha P_1}{\mathrm{i}\alpha F_r^2 - P_0}, \tag{3.18e,f}$$

$$b_{40} = \frac{P_0}{\mathrm{i}\alpha F_r^2 - P_0}, \qquad b_{41} = F_r^2\frac{\mathrm{i}\alpha P_1}{\mathrm{i}\alpha F_r^2 - P_0}, \tag{3.18g,h}$$

$$P_0 = \frac{1}{a_{11} - a_{14}}\left[(\mathrm{i}\alpha)^2 - \frac{a_{11}a_{23}^2}{a_{22}}\right], \qquad P_1 = \frac{a_{15}}{a_{11} - a_{14}}. \tag{3.18i,j}$$

On substituting from (3.14*c*) and (3.17) into the sediment continuity equation (3.8) we obtain the following differential equation:

$$f_0\hat{\eta}_{1,t} + L_{a0}\hat{f}_{1,t} = [\Gamma_F\hat{f}_1 + f_0(\Gamma_\phi\hat{\phi}_{g1} + \Gamma_\sigma\hat{\sigma}_1 + \Gamma_\eta\hat{\eta}_1)], \tag{3.19}$$

where

$$\Gamma_\phi = -\Phi_0\{\mathrm{i}\alpha(2b_{11} + b_{41}C_D)q_\eta + \mathrm{i}\alpha q_\phi - \tfrac{1}{2}\pi b_{21}\}, \tag{3.20a}$$

$$\Gamma_\sigma = \Phi_0\{\mathrm{i}\alpha(2b_{11} + b_{41}C_D)q_\eta - \mathrm{i}\alpha q_\sigma - \tfrac{1}{2}\pi b_{21}\}, \tag{3.20b}$$

$$\Gamma_F = -\mathrm{i}\alpha\Phi_0, \quad \Gamma_\eta = -\Phi_0\left\{\mathrm{i}\alpha(2b_{10} + b_{40}C_D)q_\eta + \tfrac{1}{2}\pi\left(-b_{20} + R\tfrac{1}{2}\pi\right)\right\}. \tag{3.20c,d}$$

Finally, integrating (3.19) over the grain size and imposing the integral condition (2.2), which at order ε requires that

$$\int_{-\infty}^{\infty}\hat{f}_1\,\mathrm{d}\phi = 0, \tag{3.21}$$

we obtain the equation

$$\hat{\eta}_{1,t} = \left[\hat{\phi}_{g1}\int_{-\infty}^{\infty}f_0\Gamma_\phi\,\mathrm{d}\phi + \hat{\sigma}_1\int_{-\infty}^{\infty}f_0\Gamma_\sigma\,\mathrm{d}\phi + \int_{-\infty}^{\infty}\hat{f}_1\Gamma_F\,\mathrm{d}\phi + \hat{\eta}_1\int_{-\infty}^{\infty}f_0\Gamma_\eta\,\mathrm{d}\phi\right]. \tag{3.22}$$

Substituting $\hat{\eta}_{1,t}$ from (3.22) into (3.19) we find

$$\begin{aligned} L_{a0}\hat{f}_{1,t} = {} & \left\{f_0\left[\Gamma_\phi - \int_{-\infty}^{\infty}f_0\Gamma_\phi\,\mathrm{d}\phi\right]\hat{\phi}_{g1} + f_0\left[\Gamma_\sigma - \int_{-\infty}^{\infty}f_0\Gamma_\sigma\,\mathrm{d}\phi\right]\hat{\sigma}_1\right. \\ & \left. + \left[\hat{f}_1\Gamma_F - f_0\int_{-\infty}^{\infty}\Gamma_F\hat{f}_1\,\mathrm{d}\phi\right] + f_0\left[\Gamma_\eta - \int_{-\infty}^{\infty}f_0\Gamma_\eta\,\mathrm{d}\phi\right]\hat{\eta}_1\right\}. \end{aligned} \tag{3.23}$$

We then obtain a system of two coupled integro-differential equations (3.22), (3.23) that constitute the main result of linear analysis. Equation (3.22) suggests that sediment heterogeneity does affect bar instability through several contributions. In

fact, if we neglect the effect of heterogeneity of the sediment, which implies that $\hat{f}_1$ vanishes, (3.22) reduces to the usual equation which governs the linear growth of bar perturbations with uniform sediments, namely

$$\hat{\eta}_{1,t} = (\Omega - \mathrm{i}\omega)\hat{\eta}_1, \tag{3.24}$$

where $\Omega - \mathrm{i}\omega$ is the complex growth rate. Moreover, bottom topography affects the spatial distribution of grain size through the fourth term appearing in (3.23). Also, note that the unknown variables in (3.22), (3.23) are $\hat{\eta}_1$ and $\hat{f}_1$, since $\hat{\phi}_{g1}$ and $\hat{\sigma}_1$ are related to $\hat{f}_1$ through (3.4*c*, *d*). The procedure can be readily generalized to account for any moment of grain size distribution.

4. Analytical solution

The two integro-differential equations (3.22), (3.23) which govern the growth of perturbations of bottom elevation and grain size distribution can be solved numerically. However, an analytical treatment is possible for the case of a mixture composed of N different discrete sizes, following a procedure similar to that adopted by Seminara *et al.* (1996). We then assume the probability density function f to be represented in terms of a sum of N delta Dirac functions $\delta(\phi - \phi_i)$, each centred on ϕ_i, yielding

$$[f_0(\phi), \hat{f}_1(\phi, t)] = \sum_{i=1}^{N} \{[f_{0i}, \hat{f}_{1i}(t)]\delta(\phi - \phi_i)\}. \tag{4.1}$$

We reformulate definitions (3.4*c*, *d*) into the discrete forms

$$\hat{\phi}_{g1}(t) = \sum_{i=1}^{N} \hat{f}_{1i}(t)\phi_i, \quad \hat{\sigma}_1(t) = \frac{1}{2\sigma_0} \sum_{i=1}^{N} [\hat{f}_{1i}(t)(\phi_i - \phi_{g0})^2]. \tag{4.2a,b}$$

On substituting from (4.1) and (4.2) into (3.22) we obtain

$$\hat{\eta}_{1,t} = \left[\sum_{i=1}^{N} (\hat{f}_{1i}\phi_i)\Sigma_1 + \frac{1}{2} \sum_{i=1}^{N} [\hat{f}_{1i}(\phi_i - \phi_{g0})^2]\, \Sigma_2 + \hat{\eta}_1 \Sigma_3 + \sum_{i=1}^{N} (\hat{f}_{1i}\Gamma_{Fi}) \right], \tag{4.3}$$

where

$$\Sigma_1 = \sum_{i=1}^{N} \left(f_{0i}\Gamma_{\phi i}\right), \quad \Sigma_2 = \sum_{i=1}^{N} \left(f_{0i}\Gamma_{\sigma i}\right), \quad \Sigma_3 = \sum_{i=1}^{N} \left(f_{0i}\Gamma_{\eta i}\right), \tag{4.4a–c}$$

and the following notation is adopted:

$$(\Gamma_{\phi i}, \Gamma_{\sigma i}, \Gamma_{Fi}, \Gamma_{\eta i}) = \left[\Gamma_\phi(\phi_i), \Gamma_\sigma(\phi_i), \Gamma_F(\phi_i), \Gamma_\eta(\phi_i)\right]. \tag{4.5}$$

Equation (3.23) evaluated at discrete points ϕ_i $(i = 1, 2, \ldots, N-1)$ provides $(N-1)$ equations describing the time evolution of the $(N-1)$ perturbations $\hat{f}_{1i}(t)$ of the grain size distribution function

$$\hat{f}_{1i,t} = \frac{1}{L_{a0}} \Bigg\{ f_{0i}[\Gamma_{\phi i} - \Sigma_1] \sum_{j=1}^{N} (\hat{f}_{1j}\phi_j) + f_{0i}[\Gamma_{\sigma i} - \Sigma_2] \frac{1}{2\sigma_0} \sum_{j=1}^{N} [\hat{f}_{1j}(\phi_j - \phi_{g0})^2] + \left[\hat{f}_{1i}\Gamma_{Fi} - f_{0i} \sum_{j=1}^{N} (\Gamma_{Fj}\hat{f}_{1j}) \right] + f_{0i}[\Gamma_{\eta i} - \Sigma_3]\hat{\eta}_1 \Bigg\}. \tag{4.6}$$

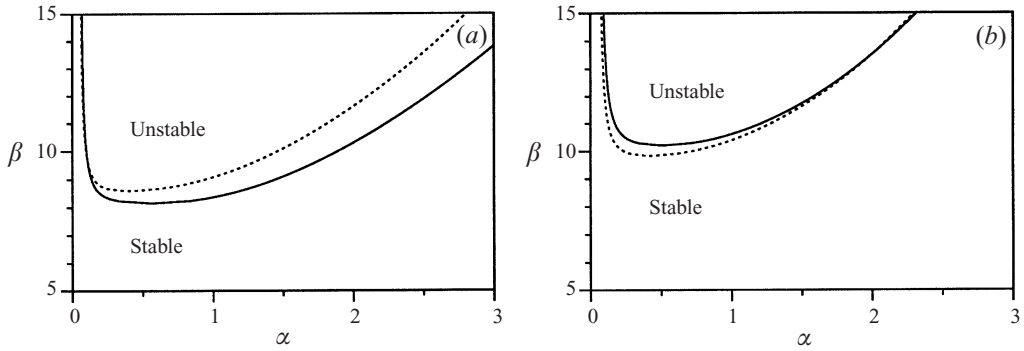

FIGURE 2. Examples of neutral curves for alternate bar formation in the case of a bimodal mixture ($d_{g0} = 0.01$; $\sigma_0 = 2$): (*a*) $\Theta_{g0} = 0.07$; (*b*) $\Theta_{g0} = 0.10$. The corresponding curves for the uniform sediment case are also reported (dotted lines).

We then obtain a linear algebraic eigenvalue problem if we write

$$(\hat{\eta}_1, \hat{f}_{1i}) = \sum_{k=1}^{N} (\mathrm{e}^{(k)}, \varphi_i^{(k)}) \exp(c_k t), \tag{4.7}$$

where $c_k = \Omega_k - \mathrm{i}\omega_k$ is the kth eigenvalue, with Ω_k and ω_k denoting the growth rate and the angular frequency of perturbations, while $(e^{(k)}, \varphi_1^{(k)}, \varphi_2^{(k)}, \ldots)$ is the kth eigenvector.

Note that if we set $e^k = 0$ we reduce the system (4.3), (4.4) to the eigenvalue problem for the bedload sheet case. The uniform sediment case is easily recovered by setting $N = 1$ and leads to a dispersion relationship of the form (Colombini *et al.* 1987)

$$\mathscr{F}(\Omega, \omega, \alpha, \beta, \Theta_{g0}, d_{g0}) = 0, \tag{4.8}$$

which for given values of the unperturbed Shields stress and dimensionless geometric mean size (Θ_{g0}, d_{g0}) allows one to define neutral conditions as those corresponding to vanishing amplification factor Ω. In the plane (α, β) this condition determines a neutral curve exhibiting a minimum which defines the critical value of width ratio β_c above which bars are expected to grow and the wavelength $L_c = 2\pi\alpha_c$ of fastest growing perturbations (see figure 2).

In the case of a graded mixture made of N discrete sizes, substituting from (4.7) into (4.3), (4.6) we obtain a dispersion relationship for N eigenvalues. Though the solution of the general case can be readily obtained, it proves to be more convenient to analyse the simplest case of a bimodal mixture ($N = 2$). The dispersion relationship then reads

$$(\Omega - \mathrm{i}\omega) = \tfrac{1}{2}\{(\psi_{11} + \psi_{22}) \pm \sqrt{(\psi_{11} - \psi_{22})^2 + 4\psi_{12}\psi_{21}}\}, \tag{4.9}$$

where

$$\psi_{11} = \frac{1}{L_{a0}}\left\{ f_{01}[\Gamma_{\phi 1} - (f_{01}\Gamma_{\phi 1} + f_{02}\Gamma_{\phi 2})](\phi_1 - \phi_2) + [\Gamma_{F1} - f_{01}(\Gamma_{F1} - \Gamma_{F2})] \right.$$
$$\left. + f_{01}[\Gamma_{\sigma 1} - (f_{01}\Gamma_{\sigma 1} + f_{02}\Gamma_{\sigma 2})] \frac{1}{2\sigma_0}[(\phi_1 - \phi_{g0})^2 - (\phi_2 - \phi_{g0})^2] \right\}, \tag{4.10a}$$

$$\psi_{12} = \frac{f_{01}}{L_{a0}}[\Gamma_{\eta 1} - (f_{01}\Gamma_{\eta 1} + f_{02}\Gamma_{\eta 2})], \tag{4.10b}$$

$$\psi_{21} = (f_{01}\Gamma_{\phi 1} + f_{02}\Gamma_{\phi 2})(\phi_1 - \phi_2) + (\Gamma_{F1} - \Gamma_{F2}) + (f_{01}\Gamma_{\sigma 1} + f_{02}\Gamma_{\sigma 2})\frac{1}{2\sigma_0}[(\phi_1 - \phi_{g0})^2 - (\phi_2 - \phi_{g0})^2], \quad (4.10c)$$

$$\psi_{22} = f_{01}\Gamma_{\eta 1} + f_{02}\Gamma_{\eta 2}. \quad (4.10d)$$

Examples of marginal curves for a bimodal mixture are reported in figure 2 for different values of the Shields parameter. The comparison with the corresponding curves of the uniform sediment case (dotted lines in the figure) suggests that sediment heterogeneity slightly modifies the region of occurrence of bars and may lead to widening or narrowing of the unstable region depending upon the value of Shields stress. A detailed discussion of the effect of sorting on bar stability is deferred to the next section.

It is worth pointing out that in the case of mixtures the dispersion relationship depends not only on Θ_{g0} and d_{g0} but also on the standard deviation of the mixture. Also note that for a bimodal mixture composed of an equal percentage of the two fractions the quantity $[(\phi_1 - \phi_{g0})^2 - (\phi_2 - \phi_{g0})^2]$ appearing in the coefficients ψ_{11} and ψ_{22} vanishes.

In general the dispersion relationship (4.9) provides two different eigenvalues. The first, namely the one obtained by choosing the positive square root, recovers the eigenvalue of the uniform sediment case as the variance of the mixture tends to vanish, while the second degenerates into a purely imaginary solution. When the perturbation of bottom amplitude is neglected the latter eigenvalue reduces to the bedload sheet mode investigated by Seminara *et al.* (1996). In this case the analysis of the limiting case of weak sorting leads to similar results in that the bedload sheet mode reduces to a sorting wave that propagates downstream with vanishing growth rate. The interested reader is referred to the above paper for further details.

5. Results and discussion

As pointed out in the Introduction, some recent experimental findings seem to suggest that the topography of bars is significantly modified by sediment heterogeneity. A brief account of the experimental results obtained by Lanzoni *et al.* (1994) is given herein. The experiments were performed in a rectangular recirculating flume, 18 m long and 0.36 cm wide, located in the Laboratory of the Hydraulic Institute of Genoa University. To investigate the effect of grain sorting on the formation of alternate bars the experimental runs were repeated, under similar hydraulic conditions, using a uniform sediment made up of glass spheres with diameter 1.5 mm and mixtures of glass spheres with roughly the same mean geometric grain diameter.

Figure 3(*a*,*b*) summarizes the main results of experiments with a bimodal mixture with diameters 1 mm and 2 mm in proportion 1 : 1. According to the indexes of bimodality introduced by Wilcock (1993) and Sambrook Smith, Nicholas & Ferguson (1997), this mixture exhibits a low degree of bimodality; hence, the hiding exponent b is likely to depart only slightly from zero (see table 1). Figure 3(*a*,*b*) shows that the major and unambiguous effect of sediment heterogeneity in each run is the decrease of both height and wavelength of bars with respect to the uniform sediment case. More precisely, figure 3(*a*) suggests that the damping effect related to sediment heterogeneity increases as the Shields parameter decreases, leading to a maximum 50% reduction

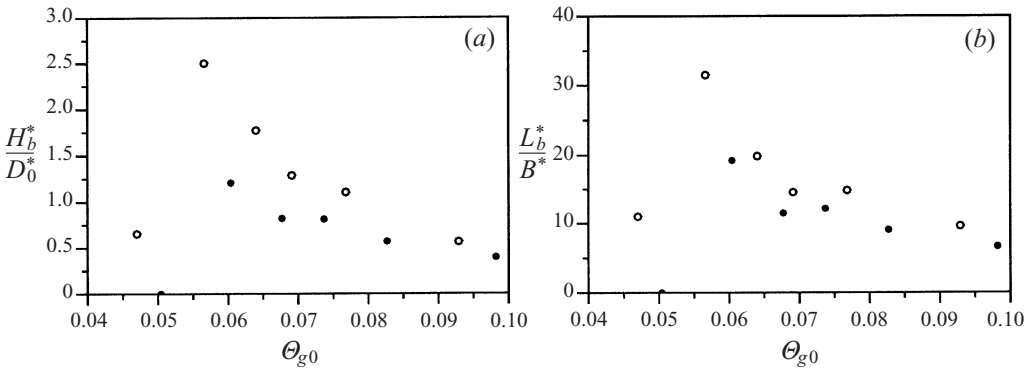

FIGURE 3. The experimental results of Lanzoni *et al.* (1994) for (*a*) bar height H_b^* and (*b*) bar wavelength L_b^* are plotted versus Shields parameter: open circles refer to experiments with glass spheres with diameter 1.5 mm; full circles refer to experiments with bimodal mixtures of glass spheres with diameters 1 mm and 2 mm.

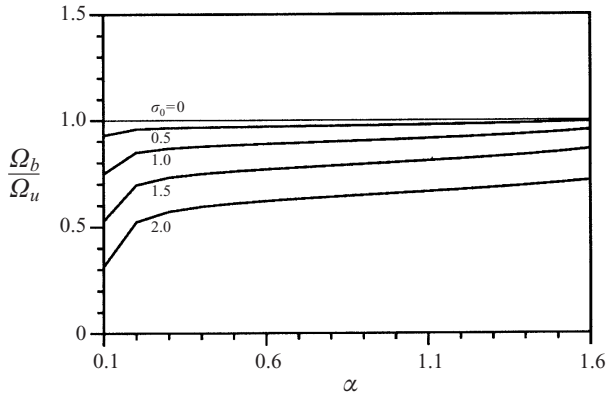

FIGURE 4. The ratio Ω_b/Ω_u between the growth rate of alternate bars for the bimodal case and for the uniform case is plotted versus bar wavenumber for different values of the standard deviation of the mixture ($d_{g0} = 0.001$; $\beta = 15$; $\Theta_{g0} = 0.08$).

of bar height when Θ_{g0} falls in the range 0.05–0.06. Moreover, the damping effect vanishes when the Shields parameter approaches the value 0.1.

The linear stability theory developed herein strictly holds for infinitesimal disturbances and therefore neglects finite-amplitude effects as well as the effect of the vertical pattern of sorting which is experimentally observed to form as bars approach their equilibrium configuration (Lanzoni 1996). In spite of these restrictions the present theoretical results are in general agreement with the experimental observations. The damping effect of sorting on bar instability is clearly exhibited by theoretical results for the growth rate of bottom perturbations reported in figure 4. Note that, for large enough values of β, damping increases as the standard deviation of the mixture increases. Also, note that theoretical results for the growth rate include the effect of the variation of the overall sediment flux, which is found to increase slightly in the case of the mixture, thus implying a small amplifying contribution to Ω.

In figure 5 the maximum growth rate is plotted versus β for some values of the mean geometric diameter and different values of the unperturbed Shields stress. The figure allows a comparison between the results of the bimodal mixture and those

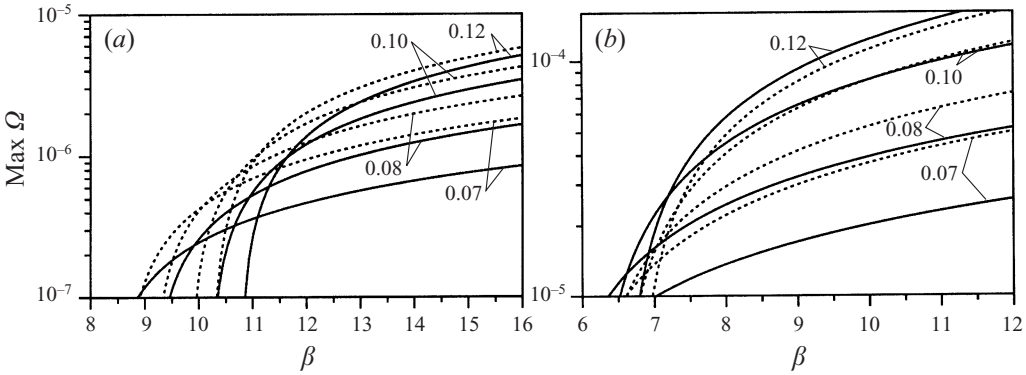

FIGURE 5. The theoretical values of the maximum growth rate of bars are plotted versus β for some values of Θ_{g0} and $\sigma_0 = 2$. The corresponding theoretical curves for the uniform sediment case are also reported (dotted lines): (*a*) $d_{g0} = 0.001$; (*b*) $d_{g0} = 0.01$.

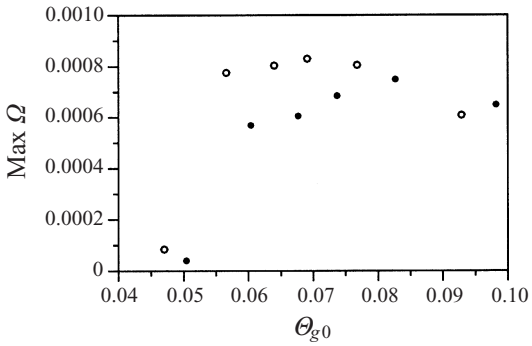

FIGURE 6. Theoretical values of the maximum growth rate corresponding to the experimental data reported in figure 3(*a*). Open and full circles refer to uniform and bimodal sediments, respectively. The calculations have been carried out by setting $b = 0.2$.

corresponding to the uniform sediment case (in the following these two cases will be referred to as bimodal and uniform, respectively, and will be denoted by the subfixes b and u). In the uniform case we have used the geometric grain diameter d_{g0} of the bimodal mixture to compute the bedload function, while we have set the bottom grain roughness equal to $n_\sigma d_\sigma$ in order to keep the same friction coefficient C as the bimodal case. Figure 5 suggests that, while sediment heterogeneity affects the threshold value of β for bar instability only slightly, a significant damping of the growth rate of bar perturbations generally occurs. Reduction of the growth rate is larger for smaller values of Shields stress and of grain roughness. As the latter parameters increase, the effect of sorting may also become slightly destabilizing, as indicated in figure 5(*b*). However, for given values of Shields stress and grain roughness, a value of $\beta > \beta_c$ always exists such that the maximum growth rate predicted by linear theory in the bimodal case falls below the value corresponding to the uniform case. As Θ_{g0} and d_{g0} decrease, this threshold value of β approaches β_c.

Figure 6 reports the theoretical values of the maximum growth rate corresponding to the experimental results summarized in figure 3(*a*), hence allowing an indirect comparison between theoretical predictions and experimental findings. It appears that the overall effect of sediment heterogeneity is adequately reproduced by the

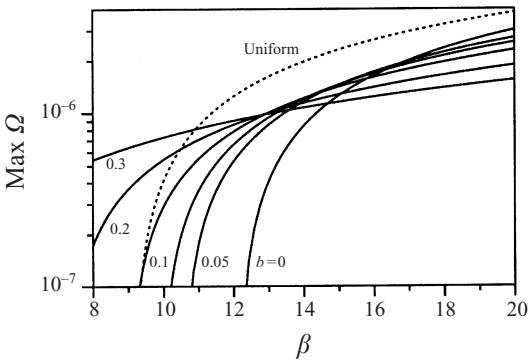

FIGURE 7. The maximum growth rate of bar perturbations is plotted versus β for different values of the exponent b of the hiding function (2.15): $\Theta_{g0} = 0.08$, $d_{g0} = 0.001$, $\sigma_0 = 2$.

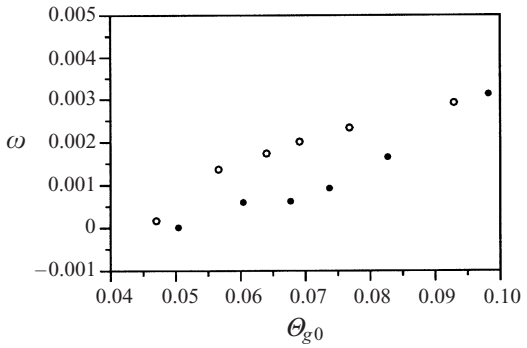

FIGURE 8. Theoretical values of the dimensionless angular frequency ω corresponding to the data reported in figure 6. Open and full circles refer to uniform and bimodal sediments, respectively. The calculations have been carried out by setting $b = 0.2$.

theoretical solution in that the damping effect is larger for low values of Θ_{g0} and vanishes when Θ_{g0} increases to a value approximately equal to 0.1.

It is worth pointing out that the effect of non-uniformity is enhanced at small values of Θ_{g0}. In fact, sorting mainly influences bar stability through the dependence of longitudinal and transverse bed load on grain size which is embodied in (2.12), (2.14) and (2.18). It can be readily seen that both contributions become vanishingly small as the Shields parameter increases: in particular, the asymptotic condition of equal mobility is progressively met at large values of Shields stress such that the function $G(\zeta)$ becomes independent of the grain size.

The magnitude of the reduction of growth rate due to sediment heterogeneity is strongly affected by the value adopted for the exponent b of the hiding function (2.15). Data reported in figures 4 and 5 are obtained with $b = 0.1$, which implies that a small (but significant) deviation from equal mobility is accounted for. When the exponent b is increased within the range of observed values, the effect of sorting on the growth rate of bars becomes invariably stabilizing, as suggested by figure 7. This also indicates that the unequal response of grain sizes in a mixture to spatial variation of bottom stress, whose effect is magnified when b is fairly large, constitutes the main stabilizing ingredient of the present analysis. This result will be more fully discussed below.

A further notable feature of the linear solution is that theoretical results seem to

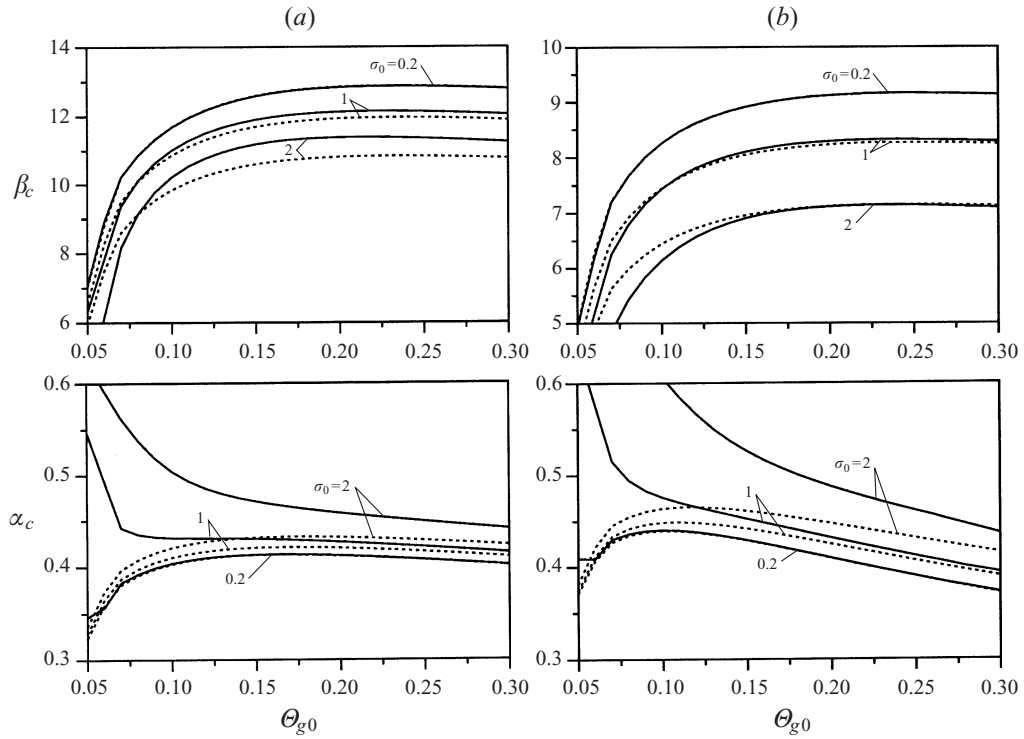

FIGURE 9. The critical values of width ratio β_c and bar wavenumber α_c predicted by linear theory are plotted versus Shields parameter for some values of σ_0 and d_{g0}. The corresponding curves for the uniform case are also reported (dotted lines): (*a*) $d_{g0} = 0.001$; (*b*) $d_{g0} = 0.01$.

reproduce the tendency of sediment heterogeneity to prevent downstream migration of bars, which has been observed by Lisle *et al.* (1991) in flume experiments characterized by shallow depth and widely graded sediments. Indeed, the theoretical values of the angular frequency, reported in figure 8 and corresponding to the experimental results of Lanzoni *et al.* (1994), support the idea that mixed-size sediments might appreciably inhibit bar migration.

Figure 9 allows a comparison between the critical values of the wavelength and width ratio (i.e. the values corresponding to the minimum of a given neutral stability curve) calculated both for the bimodal mixture and for the uniform sediment. It turns out that grain sorting leads to a reduction of the wavelength selected by the instability process, in agreement with experimental findings. Moreover, figure 9 clearly shows that the effect of sorting on β_c is fairly weak. Stabilizing effects prevail for larger values of Θ_{g0}, while β_c may be reduced due to sorting when the Shields stress approaches its threshold value.

A closer comparison between predicted and observed bar wavelengths is difficult even in the case of uniform sediment owing to the flatness of the marginal stability curve, which implies that a relatively wide range of wavenumbers is characterized by almost identical growth rates (see figure 4 of Colombini *et al.* 1987). Note, however, that in Lanzoni *et al.*'s (1994) experiments the relative shortening of bar length with respect to the case of uniform sediment varies between 0.16 and 0.42, with an average value of 0.32, while for the same set of data predicted values fall in the range 0.21–0.56, with an average value of 0.42.

We now attempt to provide a physical interpretation of the experimental and theoretical results discussed above. We assume the bottom perturbation $\hat{\eta}_1$ to be purely real, which implies that we set the origin of the s-axis in the section where, for $n = 1$, the maximum bed elevation occurs. Whence, the linear solution can be written in the form

$$\{U_1, D_1, H_1, Q_{s1}\} = \{|u_1|, |d_1|, |h_1|, |q_{S1}|\} \sin\left(\tfrac{1}{2}\pi n\right) \exp(\Omega t) \left\{ \begin{array}{l} \cos(\alpha s - \omega t - \delta_u) \\ \cos(\alpha s - \omega t - \delta_d) \\ \cos(\alpha s - \omega t - \delta_h) \\ \cos(\alpha s - \omega t - \delta_{q_s}) \end{array} \right\}, \tag{5.1a}$$

$$\{V_1, Q_{n1}\} = \{|v_1|, |q_{n1}|\} \cos\left(\tfrac{1}{2}\pi n\right) \exp(\Omega t) \left\{ \begin{array}{l} \cos(\alpha s - \omega t - \delta_v) \\ \cos(\alpha s - \omega t - \delta_{q_n}) \end{array} \right\}, \tag{5.1b}$$

$$\{\eta_1, f_1\} = \{e, |\varphi|\} \sin(\tfrac{1}{2}\pi n) \exp(\Omega t) \left\{ \begin{array}{l} \cos(\alpha s - \omega t) \\ \cos(\alpha s - \omega t - \delta_\varphi) \end{array} \right\}, \tag{5.1c}$$

where δ_i denotes the phase lag between the bed profile and a given variable. For a bimodal mixture the sediment balance equation (4.3) leads to the following relationship for the growth rate:

$$\Omega = \tfrac{1}{2}\pi \frac{|q_{n1}|}{e} \cos(\delta_{q_n}) - \frac{\alpha |q_{s1}|}{e} \sin(\delta_{q_s}) - \frac{\alpha |q_\varphi|}{e} \sin(\delta_{q_\varphi}), \tag{5.2}$$

where

$$q_\varphi = \varphi_1(\Phi_{01} - \Phi_{02}), \quad q_{s1} = f_{01}\, q_{s1} + f_{02}\, q_{s2}, \quad q_{n1} = f_{01}\, q_{n1} + f_{02}\, q_{n2}. \tag{5.3a–c}$$

Note that retaining only the first two terms on the right-hand side of (5.2) we recover the uniform case investigated by Colombini *et al.* (1987). Sediment heterogeneity has a twofold effect on Ω. In fact, the different mobility of individual grain size fractions within the mixture not only modifies the sediment transport capacity, namely q_{s1} and q_{n1}, but also induces a longitudinal and transverse pattern of sorting. The resulting perturbation φ of the grain size distribution function affects in turn q_{s1} and q_{n1}; moreover, it produces a further contribution, namely the third term on the right-hand side of (5.2), which vanishes when the asymptotic condition of equal mobility (i.e. $b = 0$) holds.

Figure 10 shows a typical example of the behaviour of the various phase lags δ_i for the bimodal case as the wavenumber changes, for given values of the parameters Θ_{g0}, d_{g0}, σ_0, and β. Results for the uniform case are also reported. It appears that δ_h, δ_d, δ_v and δ_{qn} are weakly affected by sediment non-uniformity. In particular, the flow depth is nearly in opposition to the bed profile ($\delta_d \sim \pi$) while the peak of transverse velocity V_1 is located about a quarter of a wavelength ahead of the peak of bottom profile, since δ_v is slightly larger than $\pi/2$. Furthermore, the phase lag of the transverse sediment transport δ_{qn} ranges between $\pi/2$ and π, thus implying a stabilizing contribution to Ω, as indicated by (5.2). Incidentally, we may note that this stabilizing contribution increases with the transverse mode number; therefore, it inhibits preferentially the development of higher-order transverse modes.

The peak of the longitudinal sediment transport q_{s1}, as well as the peaks of U_1 and τ_{s1}, lag upstream of the bottom crests since $\pi < \delta_{qs} < 2\pi$. Consequently, the second term on the right-hand side of (5.2) is always positive, which implies a destabilizing

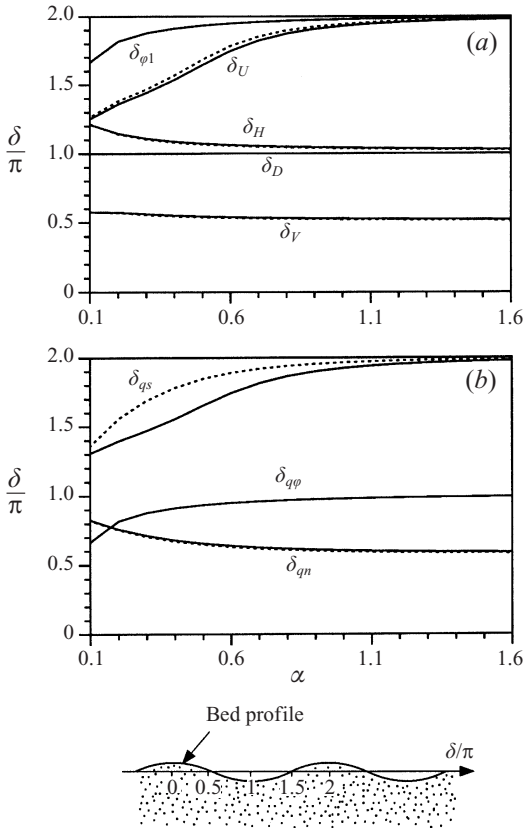

FIGURE 10. The phase lags of various flow and sediment properties with respect to bed profile are plotted versus bar wavenumber. Results for the uniform sediment case are reported as dotted lines. ($\beta = 15$; $\Theta_{g0} = 0.08$; $d_{g0} = 0.001$; $\sigma_0 = 2$).

contribution. Sediment heterogeneity leads to a reduction of δ_{qs} with respect to the uniform case, thus implying a decrease (increase) of the destabilizing contribution associated with q_{s1} depending on whether δ_{qs} is smaller (larger) than $3\pi/2$.

The effect sediment non-uniformity on the amplitude of the longitudinal and transverse components of sediment transport is illustrated in figure 11. It appears that according to (5.2) both $|q_{s1}|$ and $|q_{n1}|$ contribute to the reduction of the growth rate of bar perturbations with respect to the uniform case since $|q_{s1}|_b/|q_{s1}|_u < 1$ and $|q_{n1}|_b/|q_{n1}|_u > 1$.

The effect on $|q_{n1}|$ can be easily understood through direct inspection of (3.12*b*) which suggests that sediment non-uniformity enters into the problem through the dependence of the transport function Φ and of the coefficient R on the grain size. If we keep only the contribution related to transverse bedload, equation (5.2) reduces to the expression

$$\Omega = \tfrac{1}{4}\pi^2 \Theta_{g0}^{3/2}\{f_{01}G(\phi_1)R(\phi_1) + f_{02}G(\phi_2)R(\phi_2)\}. \tag{5.4}$$

Therefore, the stabilizing effect associated with Q_{n1} increases with respect to the uniform case according to the ratio

$$\frac{f_{01}G(\phi_1)[f_{hr}(\phi_1)]^{-1} + f_{02}G(\phi_2)[f_{hr}(\phi_2)]^{-1}}{G(\phi_{g0})},$$

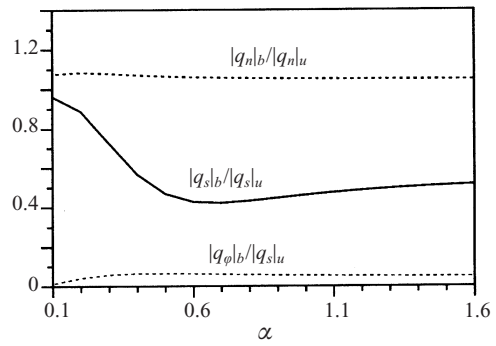

FIGURE 11. The ratio between the amplitudes of the perturbations of longitudinal and transverse components of sediment transport calculated for the bimodal case and for the uniform case is plotted versus bar wavenumber. The ratio $|q_\varphi|_b/|q_s|_u$ is also reported. ($\beta = 15; \Theta_{g0} = 0.08; d_{g0} = 0.001; \sigma_0 = 2$).

which is always greater than 1 and increases as the variance of the mixture increases.

Regarding the reduction of $|q_{s1}|$ with respect to the uniform case reported in figure 11, it is not easy to analyse separately the role played by the various terms contributing to Q_{s1} in (3.12*a*). However, we may observe that q_η, namely the contribution associated with the variation of the transport function G with respect to the Shields parameter, decreases with respect to the uniform case, the reduction being more appreciable as the Shields parameter decreases.

A direct effect of grain sorting on Ω is embodied in the third term on the right-hand side of (5.2); it appears that this contribution always induces damping of the growth rate of bar perturbations since $\pi/2 < \delta_{q\varphi} < \pi$. This stabilizing effect is essentially related to the progressive coarsening which takes place along the upstream face of bars, namely near the peak of bottom shear stress, as a consequence of the selective transport of different grain size fractions. In fact, the derivative of the sediment load function Φ with respect to the shear stress τ is such that the ratio

$$\frac{\Phi_{,\tau}|_{d_i}}{\Phi_{,\tau}|_{d_g}} = \frac{G(\phi_i)}{G(\phi_g)} \frac{\frac{3}{2} + \Gamma(\phi_i)}{\frac{3}{2} + \Gamma(\phi_g)} \tag{5.5}$$

is greater or smaller than 1, depending on whether d_i is finer or coarser than d_g, respectively. As a consequence, different grain sizes display a different response to the increasing values of bed shear stress which occur along the rising part of the bottom profile, leading to coarsening of the bed composition since finer particles are more easily transported. Indeed, figure 10 shows that the phase lag $\delta_{\varphi 1}$ of the perturbation of grain size distribution ranges between $3\pi/2$ and 2π, which implies that the coarser fraction prevails upstream of the bar crest. The above findings agree with the experimental observations of Lisle *et al.* (1991), Lisle & Madej (1992) and Lanzoni (1996).

The above tendency is counteracted by gravitational effects which tend to pull coarser particles downward selectively (see Parker & Andrews 1985). The experimental results seem to suggest that the former mechanism, namely the unequal response of grain sizes to bottom stress, prevails in the case of bars since spatial variations of bottom topography are relatively slow. It may turn out that gravity becomes the dominant mechanism which controls the location of grain sizes in the case of

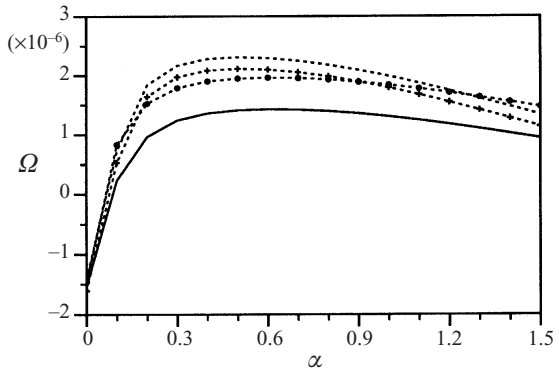

FIGURE 12. The theoretical predictions of the growth rate of alternate bars for a bimodal mixture (solid line) are compared with the values of Ω obtained in the uniform sediment case (dotted line) and with the values obtained in the bimodal case neglecting the effect of sorting on the longitudinal ($\cdots + \cdots$, $\varphi = 0$, $b = 0$) and transverse ($\cdots \bullet \cdots, f_{hr} = 0$) component of bedload: $\beta = 15$, $\Theta_{g0} = 0.08$, $d_{g0} = 0.001$, $\sigma_0 = 2$.

bedforms of smaller spatial scale, such as dunes, or when finite-amplitude effects are more prominent.

A further consequence of the sorting pattern induced by bar topography is that it implies a reduction of longitudinal sediment transport with respect to the uniform case in the region where less mobile coarser particles preferentially accumulate, namely along the upstream face of bars. Therefore, a positive contribution to $q_{s,s}$ is generated in the neighbourhood of a bar crest, which implies a negative contribution to bottom development, according to equation (3.8).

Regarding the effects of grain sorting on the migration of bars, theoretical results support the idea, reported by Lisle *et al.* (1991), that bar coarsening is mainly responsible for the observed stabilization of bars. In fact, the effect of sediment heterogeneity on the wave speed of bars is felt essentially through the dependence of ω on the perturbation of the grain size distribution φ. From (4.3) and (5.1) we obtain

$$\omega \propto \cos(\delta_{q_\varphi}). \tag{5.6}$$

Hence, bar coarsening, which implies that $\delta_{q\varphi}$ falls in the range $\pi/2$–π as discussed above, leads to a negative contribution to the wave speed.

An example of how the various mechanisms affect the growth rate of bar perturbations is given in figure 12. From the preceeding discussion it clearly emerges that, within a fairly wide range of values of the dimensionless control parameters (Θ_{g0}, d_{g0} and β), various contributions related to sediment heterogeneity act simultaneously to produce an overall stabilizing effect on bottom development, which leads to a non-negligible reduction of the depths of scour and deposition associated with bar formation, and a damping of migration speed. This is the main practical implication of the present work, which mostly applies to gravel bed rivers. The theoretical model presented herein seems to reproduce adequately the main features of bar development related to the heterogeneous character of sediments which have been observed experimentally, namely the overall stabilizing effect on bar height, the shortening of bar wavelengths, the decrease of migration speed, as well as the pattern of sorting induced by bottom development.

However, predicting the equilibrium bar morphology would require that the assumption of small perturbations be removed. To this end the development of a sound

model for vertical sorting is required as the first step to incorporate in the analysis finite-amplitude effects on the sorting process. Furthermore, the introduction of suspended load effects may allow the extension of the theory to the case when the grain size distribution includes the sand range. In this case it is possible that the effect on bed stability of sediment heterogeneity may become even more pronounced due to the strong selective character of suspended load.

This work has been financially supported by the Italian Ministry of Scientific Research (MPI 40% National Project 'Trasporto di sedimenti ed evoluzione morfologica di corsi d'acqua, estuari e lagune alle diverse scale temporali' and COFIN '97 'Morfodinamica Fluviale e Costiera'). It is a pleasure to thank P. J. Ashworth for his thorough and constructive review.

REFERENCES

Andrews, E. D. & Erman, D. C. 1986 Persistence in the size distribution of surficial bed material during an extreme snowmelt flood. *Water Resour. Res.* **22**, 191–197.

Andrews, E. D. & Parker, G. 1987 Formation of a coarse surface layer as the response to gravel mobility. In *Sediment Transport in Gravel-Bed Rivers* (ed. C. R. Thorne, J. C. Bathurst & R. D. Hey), pp. 269–325. John Wiley.

Armanini, A. 1995 Non-uniform sediment transport: dynamics of the active layer. *J. Hydraul. Res.* **33**, 611–622.

Ashida, K. & Michiue, M. 1972 Study on hydraulic resistance and bedload transport rate in alluvial streams. *Trans. JSCE* **206**, 59–69.

Ashworth, P. J. & Ferguson, R. I. 1989 Size-selective entrainment of bedload in gravel bed streams. *Water Resour. Res.* **25**, 627–634.

Ashworth, P. J., Ferguson, R. I., Ashmore, P. E., Paola, C., Powell, D. M. & Prestegaard, K. L. 1992*a* Measurements in a braided river chute and lobe, 2, sorting of bedload during entrainment, transport and deposition. *Water Resour. Res.* **28**, 1887–1896.

Ashworth, P. J., Ferguson, R. I. & Powell, M. D. 1992*b* Bedload transport and sorting in braided channels. In *Dynamics of Gravel-Bed Rivers* (ed. P. Billi, R. D. Hey, C. R. Thorne & P. Tacconi), pp. 497–513. John Wiley.

Bagnold, R. A. & Barndorff-Nielsen, O. E. 1980 The pattern of natural size distributions. *Sedimentology* **27**, 199–207.

Buffington, J. M. & Montgomery, D. R. 1997 A systematic analysis of eight decades of incipient motion studies, with special reference to gravel-bedded rivers. *Water Resour. Res.* **33**, 1993–2029.

Callander, R. A. 1969 Instability of river channels. *J. Fluid Mech.* **36**, 465–480.

Christiansen, C. & Hartmann, D. 1991 The hyperbolic distribution. In *Principles, Methods, and Application of Particle Size Analysis* (ed. J. P. M. Syvitski), pp. 264–279. Cambridge University Press.

Colombini, M., Seminara, G. & Tubino, M. 1987 Finite-amplitude alternate bars. *J. Fluid Mech.* **181**, 213–232.

Colombini, M. & Tubino, M. 1991 Finite-amplitude free-bars: a fully nonlinear spectral solution. In *Sand Transport in Rivers, Estuaries and the Sea* (ed. R. Soulsby & R. Bettes). *Proc. Euromech 262 Colloquium, Wallingford, UK, 26-19 June*, p. 213. Balkema.

Diplas, P. 1987 Bedload transport in gravel-bed streams. *J. Hydraul. Engng ASCE* **113**, 277–292.

Diplas, P. & Parker, G. 1992 Deposition and removal of fines in gravel-bed streams. In *Dynamics of Gravel-Bed Rivers* (ed. P. Billi, R. D. Hey, C. R. Thorne & P. Tacconi), pp. 313–326. John Wiley.

Egiazaroff, I. V. 1965 Calculations of nonuniform sediment concentrations. *J. Hydraul. Div. ASCE* **91**, 225–247.

Ferguson, R. I. 1994 Critical discharge for entrainment of poorly sorted gravel. *Earth Surf. Processes Landforms* **19**, 179–186.

Ferguson, R. I., Prestegaard, K. L. & Ashworth, P. J. 1989 Influence of sand on hydraulics and gravel transport in a braided gravel bed river. *Water Resour. Res.* **25**, 635–643.

Fredsöe, J. 1978 Meandering and braiding of rivers. *J. Fluid Mech.* **84**, 609–624.

Garcia, M. & Niño, Y. 1993 Dynamics of sediment bars in straight and meandering channels: Experiments on the resonance phenomenon. *J. Hydraul. Res.* **31**, 739–762.

Hirano, M. 1971 River bed degradation with armouring. *Trans. JSCE* **195**, 55–65.

Ikeda, S. 1982 Lateral bed load transport on side slopes. *J. Hydraul. Div. ASCE* **108**, 1369–1373.

Kikkawa, H., Ikeda, S. & Kitagawa, A. 1976 Flow and bed topography in curved open channels, *J. Hydraul. Div. ASCE* **12**, 1327–1342.

Klaassen, G. J. 1990 Experiments with graded sediments in a straight flume. *DELFT HYDRAULICS*, *TOW Rivers*, *Rep.* Q778.

Kuhnle, R. A. 1992 Fractional transport rates of bedload on Goodwin Creek. In *Dynamics of Gravel-Bed Rivers* (ed. P. Billi, R. D. Hey, C. R. Thorne & P. Tacconi), pp. 141–155. John Wiley.

Kuroki, M. 1988 Study on flow and bedforms of alluvial rivers. PhD thesis, Hokkaido University, Japan (in Japanese).

Lanzoni, S. 1996 Experiments on free and forced bar formation in a straight flume. Vol. II: Graded sediment. *DELFT HYDRAULICS. Res. Rep.* Q1774.

Lanzoni, S., Tubino, M. & Bruno, S. 1994 Formazione di barre alternate in alvei incoerenti a granulometria non uniforme. *XXIII Convegno di Idraulica e Costruzioni Idrauliche*, *Napoli*, *II*, T4/pp. 171–181 (in Italian).

Lisle, T. E., Ikeda, H. & Iseya, F. 1991 Formation of stationary alternate bars in a steep channel with mixed size sediment: a flume experiment. *Earth Surf. Proc. Landforms* **16**, 463–469.

Lisle, T. E. & Madej, M. A. 1992 Spatial variation in armouring in a channel with high sediment supply. In *Dynamics of Gravel-Bed Rivers* (ed. P. Billi, R. D. Hey, C. R. Thorne & P. Tacconi), pp. 277–291. John Wiley.

Misri, R. L., Garde, R. J. & Ranga Raju, K. G. 1984 Bedload transport of coarse nonuniform sediment. *J. Hydraul. Engng ASCE* **110**, 312–328.

Olesen, K. W. 1987 Bed topography in shallow river bends. *Commun. on Hydraul. and Geotech. Engng n.* 87-1. Delft University of Technology, The Netherlands.

Paola, C. & Seal, R. 1995 Grain size patchiness as a cause of selective deposition and downstream fining. *Water Resour. Res.* **31**, 1395–1407.

Parker, G. 1976 On the cause and characteristic scale of meandering and braiding in rivers. *J. Fluid Mech.* **76**, 457–480.

Parker, G. 1978 Self-formed straight rivers with equilibrium banks and mobile bed. Part 2. The gravel river. *J. Fluid Mech.* **89**, 127–147.

Parker, G. 1984 Discussion of: Lateral bedload on side slopes. *J. Hydraul. Div. ASCE* **110**, 197–199.

Parker, G. 1990 Surface-based bedload transport relation for gravel rivers. *J. Hydraul. Res.* **28**, 417–436.

Parker, G. 1992 Some random notes on grain sorting. *Proc. Grain Sorting Seminar*, *Ascona*, Switzerland, pp. 19–76.

Parker, G. & Andrews, E. D. 1985 Sorting of bedload sediment by flow in meander bends. *Water Resour. Res.* **21**, 1361–1373.

Parker, G. & Klingeman, P. C. 1982 On why gravel bed streams are paved. *Water Resour. Res.* **18**, 1409–1423.

Proffitt, G. T. & Sutherland, A. J. 1983 Transport of non-uniform sediments. *J. Hydraul. Res.* **21**, 33–43.

Repetto, R., Tubino, M. & Zolezzi, G. 1996 Sulla formazione di barre fluviali in granulometria fine. *XXV Convegno di Idraulica e Costruzioni Idrauliche*, Torino, *II*, pp. 322–333 (in Italian).

Ribberink, J. S. 1987 Mathematical modelling of one-dimensional morphological changes in rivers with non-uniform sediment. *Commun. on Hydraul. and Geotech. Engng Rep. 87-2*, p. 200. Delft University of Technology.

Sambrook Smith, G. H., Nicholas, A. P. & Ferguson, R. I. 1997 Measuring and defining bimodal sediments: Problems and implications. *Water Resour. Res.* **33**, 1179–1185.

Schielen, R., Doelman, A. & De Swart, H. E. 1993 On the nonlinear dynamics of free bars in straight channels. *J. Fluid Mech.* **252**, 325–356.

Sekine, M. & Parker, G. 1992 Bedload transport on a transverse slope. *J. Hydraul. Div. ASCE* **118**, 513–535.

Seminara, G. 1995 Invitation to river morphodynamics. Invited lecture at '*Intl Conference on Nonlinear Dynamics and Pattern Formation in Natural Environment* (ICPF '94)', *Noordwijkerhout, NL*. Pitman Research Notes in Mathematics, vol. **335** (ed. A. Doelman & A. van Harten), pp. 269–294. Longman.

Seminara, G., Colombini, M. & Parker, G. 1996 Nearly pure sorting waves and formation of bedload sheets. *J. Fluid Mech.* **312**, 253–278.

Seminara, G. & Tubino, M. 1989 Alternate bars and meandering: free, forced and mixed interactions. In *River Meandering* (ed. S. Ikeda & G. Parker). AGU Water Resour. Monograph, vol. 12, pp. 267–320.

Sengupta, S., Ghosh, J. K. & Mazumder, B. S. 1991 Experimental-theoretical approach to interpretation of grain size frequency distributions. In *Principles, Methods, and Application of Particle Size Analysis* (ed. J. P. M. Syvitski), pp. 264–279. Cambridge University Press.

Shaw, J. & Kellerhals, R. 1982 The composition of recent alluvial gravels in Alberta river beds. *Bull. Alberta Res. Counc.* vol. **41**, Edmonton, Alberta, Canada, 151 pp.

Talmon, A. C., Struiksma, N. & Van Mierlo, M. C. L. M. 1995 Laboratory measurements of the direction of sediment transport on transverse alluvial-bed slopes. *J. Hydraul. Res.* **33**, 495–518.

Tanner, W. F. 1983 Hydrodynamic origin of Gaussian size distribution. In *Nearshore Sedimentology*: *Proc. 6th Symp. on Coastal Sedimentology* (ed. W. F. Tanner), pp. 12–34. Geology Department, Florida State Univ., Tallahassee.

Visher, G. S. 1969 Grain size distributions and depositional processes. *J. Sedimentary Petrol.* **39**, 1074–1106.

Watanabe, Y. & Tubino, M. 1992 Influence of bedload and suspended load on alternate bars. *Proc. Hydraul. Eng. ISCE*, 36.

Wathen, S. J., Ferguson, R. I., Hoey, T. B. & Werritty, A. 1995 Unequal mobility of gravel and sand in weakly bimodal river sediments. *Water Resour. Res.* **31**, 2087–2096.

White, W. R. & Day, T. J. 1982 Transport of graded bed material. In *Gravel-Bed Rivers* (ed. J. C. Bathurst & C. R. Thorne), pp. 181–224. John Wiley.

Whiting, P. J., Dietrich, W. E., Leopold, L. B. & Collins, L. 1985 The variability of sediment transport in a fine gravel stream. *Proc. Intl Fluvial Sedimentology Conf. 3rd., Fort Collins*, p. 38, Colorado State University.

Wilcock, P. R. 1987 Bed-load transport of mixed-size sediment. PhD Dissertation, 205 pp. MIT, Cambridge.

Wilcock, P. R. 1988 Methods for estimating the critical shear stress of individual fractions in mixed-sizes sediment. *Water Resour. Res.* **24**, 1127–1135.

Wilcock, P. R. 1992 Experimental investigation of the effect of mixture properties on transport dynamics. In *Dynamics of Gravel-Bed Rivers* (ed. P. Billi, R. D. Hey, C. R. Thorne & P. Tacconi), pp. 109–139. John Wiley.

Wilcock, P. R. 1993 Critical shear stress of natural sediments. *J. Hydraul. Engng* **119**, 491–505.

Wilcock, P. R. & McArdell, B. W. 1993 Surface-based fractional transport rates: Mobilization thresholds and partial transport of sand-gravel sediment. *Water Resour. Res.* **29**, 1297–1312.

Wilcock, P. R. & Southard, J. B. 1988 Experimental study of incipient motion in mixed-size sediment. *Water Resour. Res.* **24**, 1137–1151.